To appear in the *International Journal of Control*
Vol. 00, No. 00, Month 20XX, 1–24

Adaptive Suboptimal Second Order Sliding Mode Control for Microgrids

Gian Paolo Incremona*, Michele Cucuzzella, and Antonella Ferrara

Dipartimento di Ingegneria Industriale e dell'Informazione, University of Pavia, Via Ferrata 5, 27100, Pavia, Italy

(*This is the final version of the accepted paper submitted to International Journal of Control*)

*Corresponding author. Email: gp.incremona@gmail.com

This paper deals with the design of adaptive suboptimal second order sliding mode (ASSOSM) control laws for grid-connected microgrids. Due to the presence of the inverter, of unpredicted load changes, of switching among different renewable energy sources, and of electrical parameters variations, the microgrid model is usually affected by uncertain terms which are bounded, but with unknown upper bounds. To theoretically frame the control problem, the class of second order systems in Brunovsky canonical form, characterized by the presence of matched uncertain terms with unknown bounds, is first considered. Four adaptive strategies are designed, analyzed and compared to select the most effective ones to be applied to the microgrid case study. In the first two strategies the control amplitude is continuously adjusted, so as to arrive at dominating the effect of the uncertainty on the controlled system. When a suitable control amplitude is attained, the origin of the state-space of the auxiliary system becomes attractive. In the other two strategies a suitable blend between two components, one mainly working during the reaching phase, the other being the predominant one in a vicinity of the sliding manifold, is generated, so as to reduce the control amplitude in steady-state. The microgrid system in grid-connected operation mode, controlled via the selected ASSOSM control strategies, exhibits appreciable stability properties, as proved theoretically and shown in simulation.

Keywords: Adaptive control, sliding mode control, robust control, uncertain systems, power systems.

1. Introduction

The emerging presence of renewable energy sources, such as photovoltaic arrays, wind turbines, fuel cells, diesel generators, and energy storage devices, has given rise to a new concept of energy production and distribution (Lasseter, 2002; Lasseter and Paigi, 2004). Nowadays, new geographically distributed generation units (DGus) play an important role in this panorama, guaranteeing technical, economical and environmental benefits (Palizban, Kauhaniemi, and Guerrero, 2014).

In a typical DGu, the energy sources are interfaced to the main grid via pulse width modulation (PWM) voltage-sourced converters (VSC), and two different operating modes are possible: the grid-connected operation mode (GCOM) and the islanded operation mode (IOM). In GCOM, the microgrid works in current control mode and supplies the considered load, provided that the voltage amplitude is kept to the rated, i.e., nominal, value by the main grid. When the DGu is disconnected from the main grid, i.e., in IOM, it works in voltage control mode.

Several control techniques are reported in the literature to control microgrids either in GCOM or IOM. These control techniques generally uses conventional PI controllers (see Babazadeh and Karimi (2011a,b); Hamzeh, Karimi, and Mokhtari (2012); Hamzeh, Ghazanfari, Mokhtari, and Karimi (2013); Karimi, Nikkhajoei, and Iravani (2008), and the references therein cited), but also more advanced control methodologies such as droop mode control (De Brabandere, Bolsens, Van den Keybus, Woyte, Driesen, and Belmans, 2007; Lee, Chu, and Cheng, 2013; Planas, Gil-de Muro, Andreu, Kortabarria, and de Alegría, 2013), and model predictive control (Han, Solanki, and Solanki, 2013; Ouammi, Dagdougui, Dessaint, and Sacile, 2015; Parisio, Rikos, and Glielmo, 2014).

One of the crucial problems in microgrids is the presence of the VSC which can be viewed as a source of modelling uncertainty and disturbances. The uncertain terms affecting the microgrid model require that robust control laws are designed to solve the associated control problems. Sliding Mode Control (SMC) can represent a valid solution able to guarantee particularly appreciable robustness properties of the controlled systems in spite of modelling uncertainties and external disturbances (Edwards and Spurgeon, 1998; Utkin, 1992). Yet, SMC can feature the so-called chattering effect, i.e., high frequency oscillations of the controlled variable due to the discontinuities of the control law (Boiko, Fridman, Pisano, and Usai, 2007; Fridman, 1999, 2002). In the literature, several methods have been proposed to alleviate the chattering by-product. One of the most effective consists in artificially increasing the relative degree of the system and designing Higher Order Sliding Mode (HOSM) control laws (Dinuzzo and Ferrara, 2009; Levant, 2003; Shtessel, Edwards, Fridman, and Levant, 2014; Shtessel, Fridman, and Zinober, 2008). Among the HOSM control laws, those of the second order (SOSM control laws) (see, for instance Bartolini, Ferrara, and Usai (1998c); Bartolini, Ferrara, Usai, and Utkin (2000)) are particularly suitable to be applied to microgrids in grid-connected mode since the original relative degree of the microgrid model is 1. Another source of uncertainty in microgrids is the fact that only the nominal values of the parameters of the grid and of the load are typically assumed perfectly known, and their variation could be unpredictable, making the definition of the bounds on the uncertain terms impracticable.

In this paper, having in mind the grid-connected microgrid case study, the design of Adaptive Suboptimal Second Order Sliding Mode (ASSOSM) control laws is addressed. In particular, four control strategies are designed and analyzed. The first two techniques are adaptive versions of the Suboptimal SOSM (SSOSM) control presented in (Bartolini et al., 1998c), in which during the reaching phase, the control amplitude is continuously adjusted, so as to arrive at dominating the effect of the uncertainty on the controlled system. When a suitable control amplitude is attained, the origin of the state-space of the auxiliary system (i.e., the second order system with states coinciding with the sliding variable and its first time derivative) becomes finite time attractive. The other two control strategies are oriented to reduce the control amplitude in steady-state by applying an additional component to the discontinuous adaptive law, based on the "average control", obtained at the output of a first order low pass filter, in analogy with (Bartolini, Ferrara, Pisano, and Usai, 1998a). Differently than (Pisano, Tanelli, and Ferrara, 2015), the proposed strategy is not of switched

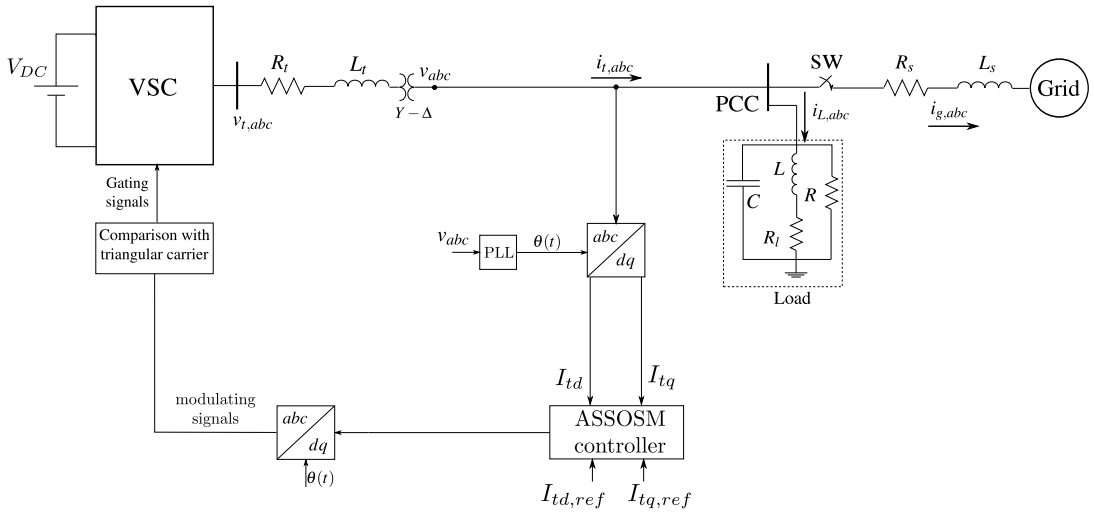

Figure 1. Simplified single-line diagram of a typical DGu.

type, and the adaptation mechanism is not based on the frequency of the sign commutations of the sliding variable when this approaches the sliding manifold. All these strategies are compared and illustrated through an academic example in order to select the most appropriate to be applied to the microgrid. The stability properties of the proposed strategies are also theoretically analyzed proving the finite time convergence of the auxiliary system states to the origin or to a vicinity of the origin of the auxiliary state-space.

Two adaptive strategies are finally applied to the considered case study. The microgrid system in GCOM controlled via the selected ASSOSM control strategies exhibits satisfactory performance even in realistic scenarios, characterized by disturbances and critical parameters variations.

Note that, sliding mode control algorithms of second and third order (which are not adaptive) have been already developed for microgrids in (Cucuzzella, Incremona, and Ferrara, 2015a,b,c).

The present paper is organized as follows. In Section 2 the microgrid case study is introduced, while in Section 3 the problem to solve is formulated. In Section 4 the proposed ASSOSM control strategies are presented. The stability analysis is reported in Section 5, while the comparison among the strategies is performed in Section 6. Simulation tests on a quite realistic DGu in GCOM are illustrated in Section 7. Some conclusions, in Section 8, end the paper.

2. The Microgrid Case Study

Consider the schematic electrical single-line diagram of a typical DGu, illustrated in Figure 1. The key element of a DGu is usually an energy source of renewable type, which can be represented by a direct current (DC) voltage source, indicated with V_{DC}. The interface medium between the DC voltage source and the main grid is realized through two components: a voltage-sourced-converter (VSC) and a filter. The first component is supposed to be a pulse width modulation (PWM) inverter, which converts DC to alternate current (AC), while the second component is a resistive-inductive filter (R_tL_t), able to extract the fundamental frequency of the VSC output voltage. Let V_d and V_q denote the direct and quadrature components of the load voltage v_{abc}, I_{td} and I_{tq} denote the direct and quadrature components of the delivered current $i_{t,abc}$. The electrical connection point of the DGu to the main grid is the so-called point of common coupling (PCC) where a local three-phase parallel resistive-inductive-capacitive load (RLC) is connected. The PCC voltage magnitude and frequency are dictated by the main grid, which is represented by a resistive-inductive line impedance (R_sL_s) and by an AC voltage source. Moreover, the presence of a phase-locked-loop (PLL) device ensures

the stiff synchronization with the grid, providing the reference angle θ for the Park's transformation (Park, 1929), and keeping the PCC quadrature voltage component V_q as close as possible to zero. Consider now the expression of the active and reactive powers, i.e.,

$$P(t) = \frac{3}{2} V_d(t) I_{td}(t), \quad Q(t) = -\frac{3}{2} V_d(t) I_{tq}(t) \tag{1}$$

Then, the DGu works in current control mode in order to supply the desired active and reactive power. According to the Park's transformation, the AC currents generated by the VSC are referred to a synchronous rotating dq-frame and regulated like DC signals. The control inputs are transformed back into the stationary abc-frame according to the inverse Park's transformation, and used to generate the gating signals through the comparison between the modulating signals and the triangular carriers (Mohan, Undeland, and Robbins, 2003). The gating signals are fed to the VSC block to generate the voltage $v_{t,abc}$ (see Figure 1). In practice, the VSC in a DGu plays the role of actuator, since its output is the control variable.

Given the DGu illustrated in Figure 1, assuming the system to be symmetric and balanced (i.e., the voltage phases are offset in time by $2\pi/3$ radians, and the impedances are equal for each phase (Mohan et al., 2003)), and applying the Kirchhoff's current (KCL) and voltage (KVL) laws, the dynamic equations modelling the considered DGu in grid-connected operation mode (GCOM) can be written in the stationary abc-frame, as follows

$$\begin{cases} i_{t,abc}(t) = \frac{1}{R} v_{abc}(t) + i_{L,abc}(t) + C \frac{dv_{abc}(t)}{dt} + i_{g,abc}(t) \\ v_{t,abc}(t) = L_t \frac{di_{t,abc}(t)}{dt} + R_t i_{t,abc}(t) + v_{abc}(t) \\ v_{abc}(t) = L \frac{di_{L,abc}(t)}{dt} + R_l i_{L,abc}(t) = L_s \frac{di_{g,abc}(t)}{dt} + R_s i_{g,abc}(t) + v_{g,abc}(t) \end{cases} \tag{2}$$

where $i_{t,abc}$ is the vector of the currents delivered by the DGu, v_{abc} is the vector of the load voltages, $i_{L,abc}$ is the vector of the currents fed into the load inductance (L), $i_{g,abc}$, and $v_{g,abc}$ are the vectors of the grid currents and grid voltages, respectively. Note that, in the following, for the sake of simplicity, the dependence of the variables on time t is omitted, when it is not strictly necessary.

Let us use, for the reader's convenience, a generic variable named s_{abc} to indicate any three-phase variable in (2). The generic s_{abc} can be referred to the synchronous rotating dq-frame by applying the Clarke's and Park's transformations as follows

$$\begin{aligned} s_{\alpha\beta} &= s_a e^{j0} + s_b e^{j\frac{2\pi}{3}} + s_c e^{j\frac{4\pi}{3}} \\ S_{dq} &= (S_d + jS_q) = s_{\alpha\beta} e^{-j\theta} \end{aligned}$$

with s being any variable in $\{i_t, v, i_L, i_g, v_t, v_g\}$, S being any variable in $\in \{I_t, V, I_L, I_g, V_t, V_g\}$, and θ provided by the PLL.

Then, the state-space representation of (2) can be expressed as

$$\begin{cases} \dot{x}_1(t) &= -\frac{1}{RC} x_1(t) + \omega x_2(t) + \frac{1}{C} x_3(t) - \frac{1}{C} x_5(t) - \frac{1}{C} x_7(t) \\ \dot{x}_2(t) &= -\omega x_1(t) - \frac{1}{RC} x_2(t) + \frac{1}{C} x_4(t) - \frac{1}{C} x_6(t) - \frac{1}{C} x_8(t) \\ \dot{x}_3(t) &= -\frac{1}{L_t} x_1(t) - \frac{R_t}{L_t} x_3(t) + \omega x_4(t) + \frac{1}{L_t} u_d(t) + \frac{1}{L_t} u_{VSC_d}(t) \\ \dot{x}_4(t) &= -\frac{1}{L_t} x_2(t) - \omega x_3(t) - \frac{R_t}{L_t} x_4(t) + \frac{1}{L_t} u_q(t) + \frac{1}{L_t} u_{VSC_q}(t) \\ \dot{x}_5(t) &= \frac{1}{L} x_1(t) - \frac{R_l}{L} x_5(t) + \omega x_6(t) \\ \dot{x}_6(t) &= \frac{1}{L} x_2(t) - \omega x_5(t) - \frac{R_l}{L} x_6(t) \\ \dot{x}_7(t) &= \frac{1}{L_s} x_1(t) - \frac{R_s}{L_s} x_7(t) + \omega x_8(t) - \frac{1}{L_s} u_{gd}(t) \\ \dot{x}_8(t) &= \frac{1}{L_s} x_2(t) - \omega x_7(t) - \frac{R_s}{L_s} x_8(t) - \frac{1}{L_s} u_{gq}(t) \\ y_d(t) &= x_3(t) \\ y_q(t) &= x_4(t) \end{cases} \tag{3}$$

where $x = [V_d\ V_q\ I_{td}\ I_{tq}\ I_{Ld}\ I_{Lq}\ I_{gd}\ I_{gq}]^T \in \mathcal{X} \subset \mathbb{R}^8$ is the state vector, $u = [V_{td}\ V_{tq}\ V_{gd}\ V_{gq}]^T \in \mathcal{U} \subset \mathbb{R}^4$ is the input vector with $u_d = V_{td}$ and $u_q = V_{tq}$, and $y = [I_{td}\ I_{tq}]^T \in \mathbb{R}^2$ is the output vector. Note that, the input $u_{gd} = V_{gd}$ and $u_{gq} = V_{gq}$ are the components of the input vector due to the presence of the main grid in the model and they are assumed to be constant to the corresponding rated, i.e., nominal, values. Furthermore, u_{VSC_d} and u_{VSC_q} are bounded Lipschitz continuous disturbances, components of the matched uncertain terms, due to the presence of the VSC as interface medium between the DGu and the main grid.

3. Problem Formulation

In order to formally state the current control problem for a grid-connected microgrid, the following sliding variables can be introduced. They are defined by considering the error of I_{td} and I_{tq} with respect to their references, i.e.,

$$\sigma_d(t) = y_{d,ref}(t) - y_d(t) \tag{4}$$
$$\sigma_q(t) = y_{q,ref}(t) - y_q(t) \tag{5}$$

where $y_{i,ref}(t)$, $i = d, q$, are assumed to be of class C with Lipschitz continuous first time derivative. By regarding the sliding variable in (4)-(5) as relevant system outputs, it appears that their relative degrees (i.e., the minimum order r of the time derivative $\sigma^{(r)}$ in which the control u explicitly appears) are equal to 1. So, a first order sliding mode control law would be adequate to steer to zero in a finite time both σ_d and σ_q. Yet, in order to alleviate the chattering phenomenon, i.e., high frequency oscillations of the controlled variable due to the discontinuity of the control law, which can be dangerous in terms of harmonics affecting the electrical signals, a SOSM control can be applied by artificially increasing the relative degree of the system. According to the SOSM control theory (Bartolini et al., 1998c), we need to define the so-called auxiliary variables $\xi_{d,1}(t) = \sigma_d(t)$ and $\xi_{q,1}(t) = \sigma_q(t)$, so that the corresponding auxiliary systems can be expressed in Brunovsky canonical form (Isidori, 1995) as

$$\begin{cases} \dot{\xi}_{i,1}(t) = \xi_{i,2}(t) \\ \dot{\xi}_{i,2}(t) = f_i(x(t), u(t), d_i(t)) + g_i w_i(t) \\ \dot{u}_i(t) = w_i(t) \end{cases} \qquad i = d, q \tag{6}$$

where $w_i(t)$, $i = d, q$, are the first time derivatives of the actual control variables $u_i(t)$, $i = d, q$, $\xi_{i,2}(t)$, $i = d, q$, are assumed to be unmeasurable, and the functions f_i, g_i, $i = d, q$, namely

$$\begin{aligned} f_d(x(t), u(t), d_d(t)) &= -(\tfrac{1}{RL_tC} + \tfrac{R_t}{L_t^2})x_1(t) + \tfrac{2\omega}{L_t}x_2(t) \\ &+(\omega^2 + \tfrac{1}{L_tC} - \tfrac{R_t^2}{L_t^2})x_3(t) + \tfrac{2\omega R_t}{L_t}x_4(t) \\ &-\tfrac{1}{L_tC}x_5(t) - \tfrac{1}{L_tC}x_7(t) + \tfrac{R_t}{L_t^2}u_d(t) \\ &-\tfrac{\omega}{L_t}u_q(t) + \ddot{x}_{3,ref}(t) + d_d(t) \\ f_q(x(t), u(t), d_q(t)) &= -\tfrac{2\omega}{L_t}x_1(t) - (\tfrac{1}{RL_tC} + \tfrac{R_t}{L_t^2})x_2(t) \\ &-\tfrac{2\omega R_t}{L_t}x_3(t) + (\omega^2 + \tfrac{1}{L_tC} - \tfrac{R_t^2}{L_t^2})x_4(t) \\ &-\tfrac{1}{L_tC}x_6(t) - \tfrac{1}{L_tC}x_8(t) + \tfrac{\omega}{L_t}u_d(t) \\ &+\tfrac{R_t}{L_t^2}u_q(t) + \ddot{x}_{4,ref} + d_q(t) \\ g_i &= -\tfrac{1}{L_t} \qquad i = d, q \end{aligned} \tag{7}$$

are bounded for physical reasons, but uncertain since they could be evaluated only relying on the nominal (not on the actual) values of the parameters, which are typically time-varying. Note that, the sign of g_i , $i = d, q$, is known and positive. The disturbances d_d and d_q depend on u_{VSC_i}, $i = d, q$, as follows

$$\begin{aligned} d_d(t) &= \frac{R_t}{L_t^2} u_{VSC_d}(t) - \frac{\omega}{L_t} u_{VSC_q}(t) + \frac{1}{L_t} \dot{u}_{VSC_d}(t) \\ d_q(t) &= \frac{R_t}{L_t^2} u_{VSC_q}(t) + \frac{\omega}{L_t} u_{VSC_d}(t) + \frac{1}{L_t} \dot{u}_{VSC_q}(t) \end{aligned} \tag{8}$$

In this paper, to face the problem in a realistic way, we assume not to know the bounds on the uncertain terms in (7)-(8).

Now, we are in position to state the control problems solved in the paper.

Problem 1: Given the auxiliary systems (6)-(8), design bounded control laws such that a second order sliding mode is enforced in a finite time, in spite of the uncertain terms in (7)-(8), and the ignorance of their bounds.

Problem 2: Given the auxiliary systems (6)-(8), design bounded control laws such that the sliding variables and their first time derivatives are ultimately bounded in a vicinity of the origin of the auxiliary systems state-space, in spite of the uncertain terms in (7)-(8), and the ignorance of their bounds.

4. The Proposed Adaptive Suboptimal Second Order Sliding Mode Control Laws

In this section, four adaptive control strategies based on the SSOSM control algorithm (Bartolini et al., 1998c) are proposed to solve the control problems previously formulated. The strategies will be designed making reference to the auxiliary systems (6)-(8) and will produce the control laws w_i, $i = d, q$. Yet, for the sake of simplicity, the subscript $i = d, q$ will be hereafter omitted.

In the following subsections, the proposed strategies are presented and illustrated through an academic example. They are also compared in order to identify the strategies which are more appropriate to be applied to the microgrid case study.

4.1 *Strategy 1*

The first ASSOSM control strategy, proposed to steer ξ_1 and ξ_2 to zero in a finite time in spite of the uncertainties and of the ignorance of the uncertainties bounds, is very simple but effective. It allows the amplitude of the discontinuous Suboptimal control law to grow until the sliding manifold becomes an attractive subspace of the controlled system state-space. In analogy with (Bartolini et al., 1998c), the control law can be first expressed as follows

$$w(t) = w_{\text{ad}}(t) = -W_{\text{ad}}(t)\,\text{sgn}\left(\xi_1(t) - \frac{1}{2}\xi_{1_{\max}}\right) \tag{9}$$

This law does not require to measure ξ_2 (this variable is unmeasurable by assumption). In fact, the extremal values $\xi_{1_{\max}}$ can be detected by determining

$$\Delta(t) = [\xi_1(t-\delta) - \xi_1(t)]\xi_1(t) \tag{10}$$

$\delta > 0$ being an arbitrarily small time delay, and considering the change of sign of $\Delta(t)$, according to the following algorithm.

Peak Detection Algorithm (Bartolini, Ferrara, and Usai, 1998b):
Let t_0 be the initial time instant. Set $\xi_{1_{\max}} = \xi_1(t_0)$ and $\xi_1(t-\delta) = 0$, $\forall\, t < \delta$, and repeat, for any $t > t_0$, the following steps:

(1) If $\Delta(t) < 0$, then $\xi_{1_{\text{mem}}} = \xi_1(t)$, else $\xi_{1_{\text{mem}}} = \xi_{1_{\text{mem}}}$.
(2) If $\Delta(t) \leq 0$ then,
If $\{\xi_{1_{\text{mem}}}\xi_{1_{\max}} > 0\} \wedge \{|\xi_{1_{\text{mem}}}| < |\xi_{1_{\max}}|\}$ then
$\xi_{1_{\max}} = \xi_{1_{\text{mem}}}$, else $\xi_{1_{\max}} = \xi_{1_{\max}}$
else $\xi_{1_{\max}} = \xi_{1_{\text{mem}}}$.

Furthermore, let

$$\Xi_{1_{\max}} = \max\{\xi_{1_{\max_i}}\} \tag{11}$$

denote the maximum of the sequence of the values of ξ_1 stored as $\xi_{1_{\max}}$. Then, the design parameter W_{ad} can be chosen according to the following adaptation mechanism

$$\dot{W}_{\text{ad}}(t) = \begin{cases} \gamma_1|\xi_1(t)| & \text{if } |\xi_1(t)| > |\Xi_{1_{\max}}| \\ 0 & \text{otherwise} \end{cases} \tag{12}$$

where γ_1 is a positive constant arbitrarily set, and $W_{\text{ad}}(t_0) = W_{\text{ad}_0}$. Note that in (12), the increment of the control amplitude is activated only when the sliding variable tends to increase with respect to the value $\Xi_{1_{\max}}$, otherwise the previous value of W_{ad} is kept.

An alternative implementation of Strategy 1 can be based on the use of the Levant's differentiator (Levant, 1998, 2003). A first advantage of this version is that the Peak Detection Algorithm is no more necessary, which improves the stability properties of the controlled system as will be clarified in Section 5. A second advantage is that the estimate of ξ_2, obtained with high (theoretically ideal) accuracy after a finite time, can be used to improve the response promptness of the adaptive mechanism, by introducing a term depending on $|\hat{\xi}_2|$. The new formulation of (12) can be expressed as

$$\dot{W}_{\text{ad}}(t) = \begin{cases} \gamma_1|\xi_1(t)| + \gamma_2|\hat{\xi}_2(t)| & \text{if } |\xi_1(t)| > |\Xi_{1_{\max}}| \\ 0 & \text{otherwise} \end{cases} \tag{13}$$

where γ_2 is a positive constant arbitrarily set, and the estimate $\hat{\xi}_2$ is computed via the Levant's differentiator

$$\dot{\hat{\xi}}_1 = -\lambda_0|\hat{\xi}_1 - \xi_1|^{1/2}\,\text{sgn}(\hat{\xi}_1 - \xi_1) + \hat{\xi}_2 \tag{14}$$

$$\dot{\hat{\xi}}_2 = -\lambda_1\,\text{sgn}(\hat{\xi}_1 - \xi_1) \tag{15}$$

where $\hat{\xi}_1,\ \hat{\xi}_2$ are the estimated values of $\xi_1,\ \xi_2$, respectively, and $\lambda_0 = 1.5L^{1/2}$, $\lambda_1 = 1.1L, L > 0$, is a possible choice of the differentiator parameters (Levant, 1998, 2003).

Remark 1: Since the Levant's differentiator is used to determine ξ_2, the extremal values $\xi_{1_{\max}}$ can be evaluated by using, as an alternative with respect to Peak Detection Algorithm, the scheme in Figure 2, as observed in (Ferrara and Incremona, 2015). That is, $\xi_{1_{\max}}$ is stored at the time instants when $\hat{\xi}_2$ changes its sign.

Remark 2: The adaptation mechanism in (13) has the advantages previously mentioned. Its disadvantage with respect to the strategy proposed in (12) is the introduction of additional parameters to set (those of the Levant's differentiator and γ_2). Moreover, it is necessary to provide sufficient

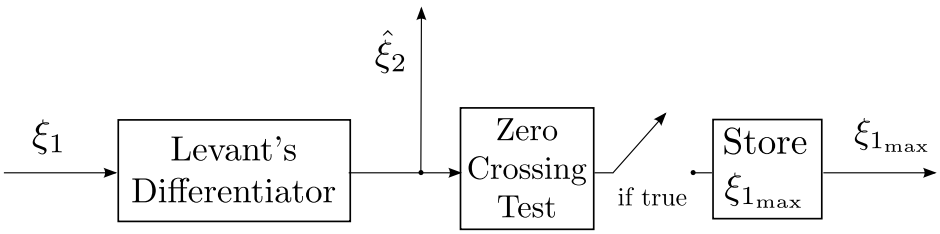

Figure 2. Representation of the peak detector.

time for the differentiator to converge (the differentiator proves to converge in a finite time), to get a usable estimate of ξ_2.

Strategy 1, in the extended version based on the Levant's differentiator, i.e., (13)-(15), will be hereafter illustrated through an academic example, consisting of a perturbed double integrator.

Example

Consider the following uncertain auxiliary system

$$\begin{cases} \dot{\xi}_1(t) = \xi_2(t) \\ \dot{\xi}_2(t) = \cos(\xi_1(t)) - \sin(\xi_1(t))\xi_2(t) + d(t) + u(t) + w(t) \end{cases} \tag{16}$$

where $d(t)$ represents an exogenous bounded disturbance. Two instances of $d(t)$ are considered, namely Disturbance 1 and Disturbance 2, as illustrated in Figure 3. Note that (16) is a system

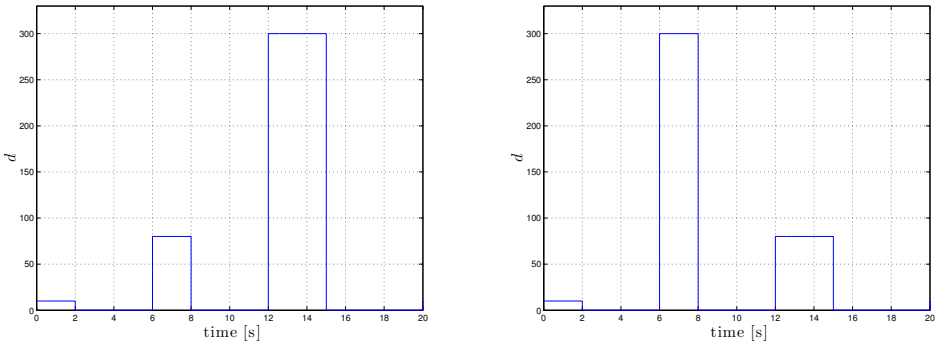

(a) (b)

Figure 3. The two instances of the matched disturbances d used in the example: (a) Disturbance 1; (b) Disturbance 2.

analogous to (6), since it can be written as

$$\begin{cases} \dot{\xi}_1(t) = \xi_2(t) \\ \dot{\xi}_2(t) = f(x(t), u(t), d(t)) + gw(t) \\ \dot{u}(t) = w(t) \end{cases} \tag{17}$$

with $f(x(t), u(t), d(t)) = \cos(\xi_1(t)) - \sin(\xi_1(t))\xi_2(t) + d(t) + u(t)$, $x(t) = [\xi_1, \xi_2]^T$, and $g = 1$. Strategy 1 in the version expressed by (13)-(15) is applied with $\gamma_1 = 30$ and $\gamma_2 = 15$. Figure 4 shows the time evolution of the adaptive gain W_{ad} for both Disturbance 1 and Disturbance 2, while Figure 5 illustrates the discontinuous control $w(t)$ and the continuous input $u(t)$, respectively. Figure 6 reports

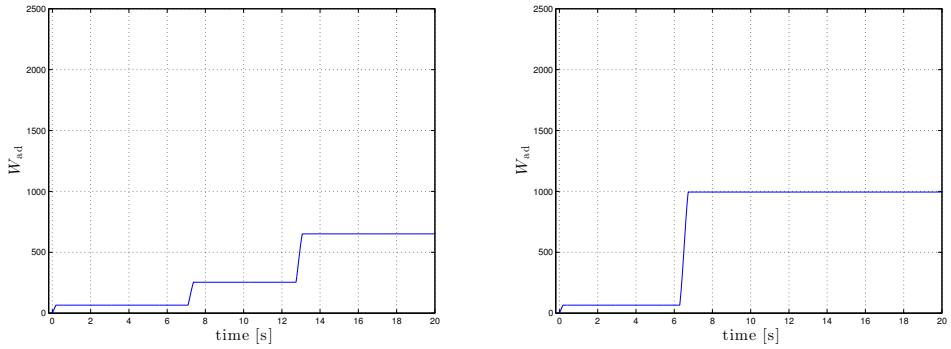

(a) (b)

Figure 4. Strategy 1: time evolution of the adaptive gain $W_{\rm ad}$: (a) in case of Disturbance 1; (b) in case of Disturbance 2.

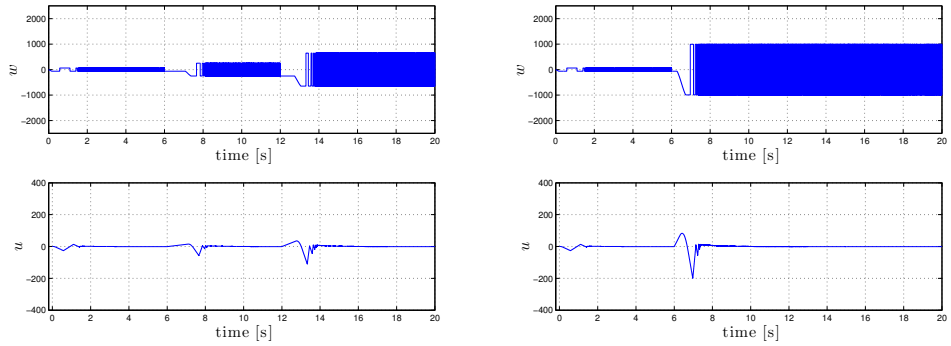

(a) (b)

Figure 5. Strategy 1: time evolution of the discontinuous auxiliary control w (top) and of the continuous input u (bottom): (a) in case of Disturbance 1; (b) in case of Disturbance 2.

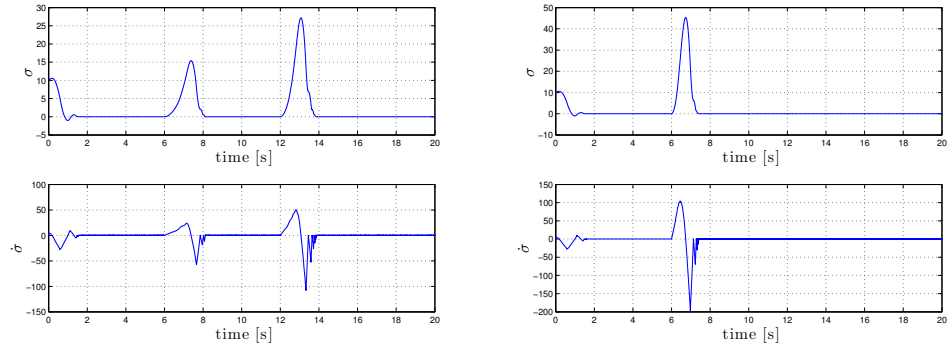

(a) (b)

Figure 6. Strategy 1: time evolution of σ and $\dot{\sigma}$: (a) in case of Disturbance 1; (b) in case of Disturbance 2.

the time evolution of the sliding variable σ and its first time derivative $\dot{\sigma}$, for both the disturbance instances.

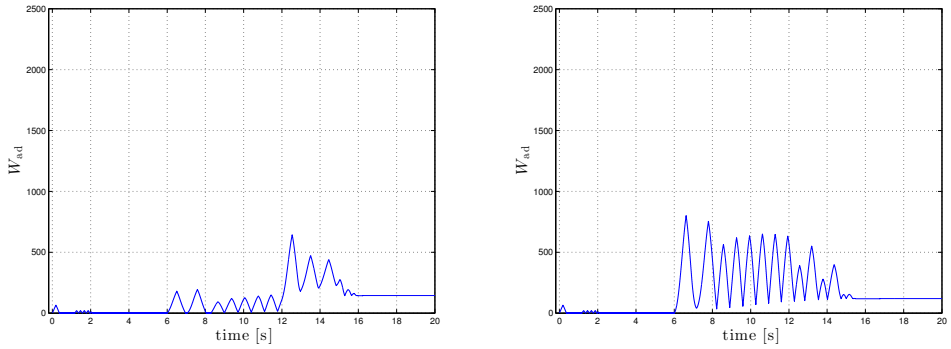

(a) (b)

Figure 7. Strategy 2: time evolution of the adaptive gain W_{ad}: (a) in case of Disturbance 1; (b) in case of Disturbance 2.

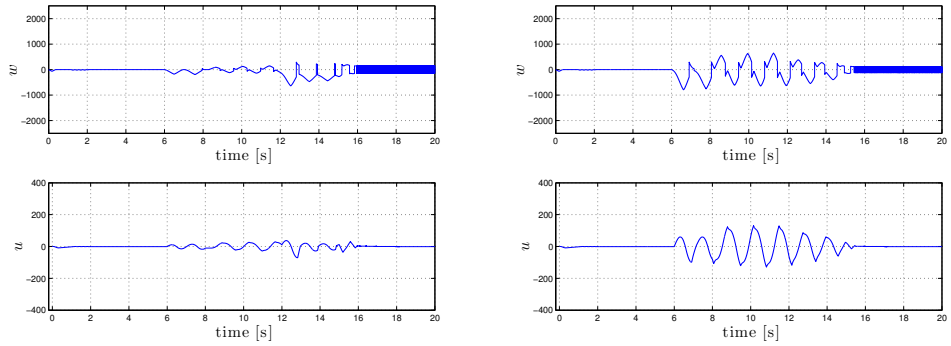

(a) (b)

Figure 8. Strategy 2: time evolution of the discontinuous auxiliary control w (top) and of the continuous input u (bottom): (a) In case of Disturbance 1; (b) In case of Disturbance 2.

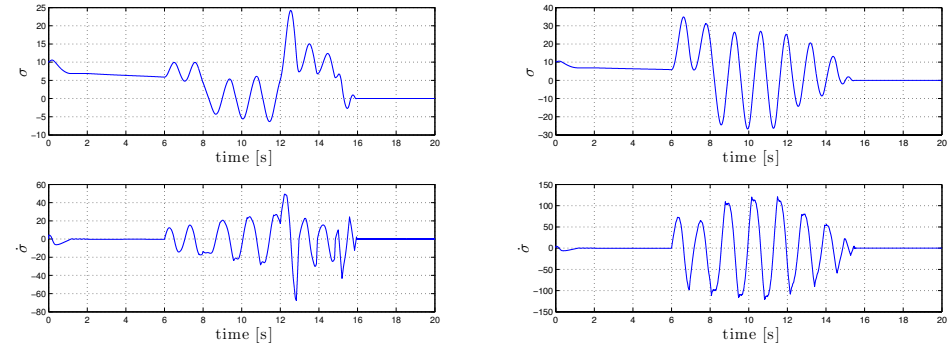

(a) (b)

Figure 9. Strategy 2: time evolution of σ and $\dot{\sigma}$: (a) in case of Disturbance 1; (b) in case of Disturbance 2.

4.2 *Strategy 2*

The adaptation mechanism proposed in Strategy 1 indicated in (12) or even in the alternative version (13), is aimed at overcoming the ignorance of the upper bound on the uncertainty terms, so transforming the ASSOSM control law into a plain SSOSM law after a transient, which is necessary for the adaptive gain to reach the appropriate size. This means that when the minimum gain to dominate the uncertainty is reached, the sliding variable is steered to zero as in a conventional

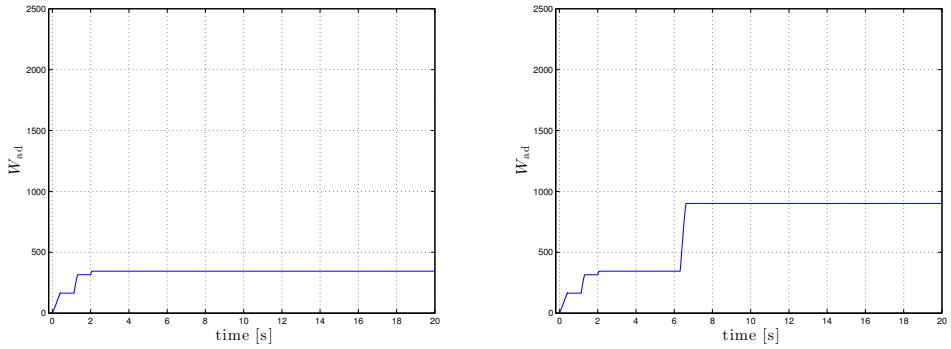

(a) (b)

Figure 10. Strategy 3: time evolution of the adaptive gain $W_{\rm ad}$: (a) in case of Disturbance 1; (b) in case of Disturbance 2.

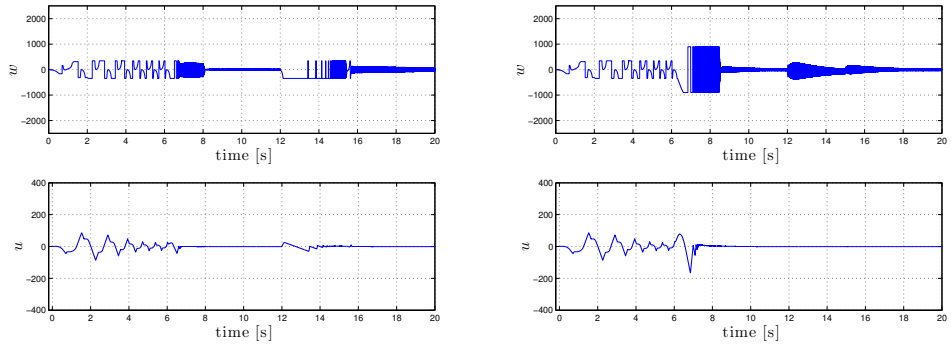

(a) (b)

Figure 11. Strategy 3: time evolution of the discontinuous auxiliary control w (top) and of the continuous input u (bottom): (a) in case of Disturbance 1; (b) in case of Disturbance 2.

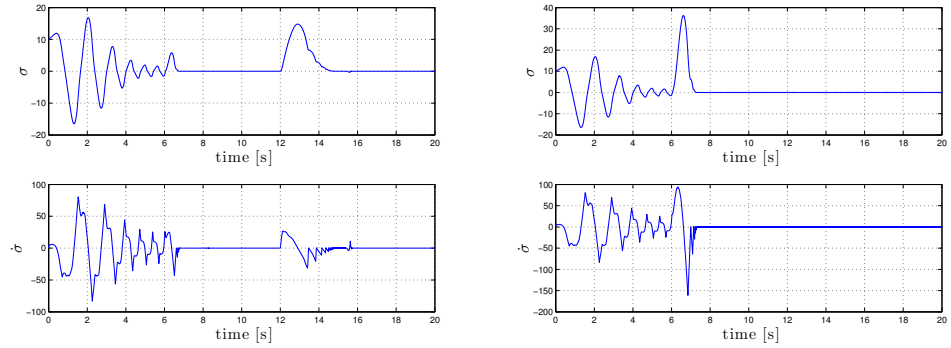

(a) (b)

Figure 12. Strategy 3: time evolution of σ and $\dot{\sigma}$: (a) in case of Disturbance 1; (b) in case of Disturbance 2.

SSOSM control law. For this reason, Strategy 1 has the same conservativeness features of the original SSOSM control algorithm. In order to decrease the control amplitude whenever the sliding variable tends towards the sliding manifold, a second adaptive SOSM control strategy can be proposed. As for Strategy 1, one could write a first version based on the Peak Detection Algorithm and a second version based on the Levant's differentiator. To keep the treatment concise, we will report hereafter only the version based on the Levant's differentiator. Specifically, the following adaptive mechanism

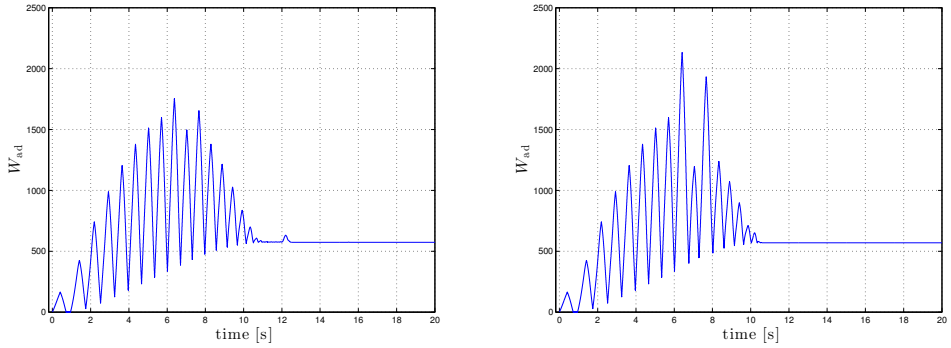

(a) (b)

Figure 13. Strategy 4: time evolution of the adaptive gain $W_{\rm ad}$: (a) in case of Disturbance 1; (b) in case of Disturbance 2.

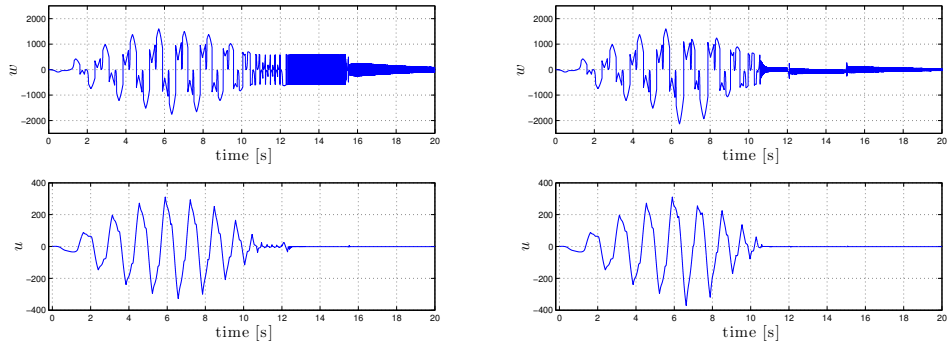

(a) (b)

Figure 14. Strategy 4: time evolution of the discontinuous auxiliary control w (top) and of the continuous input u (bottom): (a) in case of Disturbance 1; (b) in case of Disturbance 2.

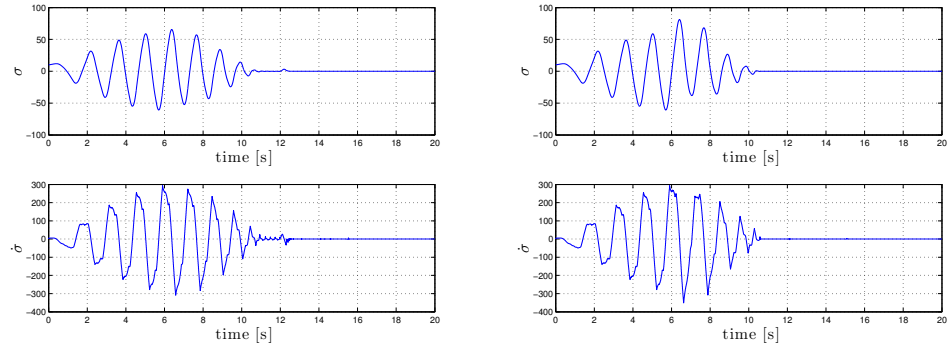

(a) (b)

Figure 15. Strategy 4: time evolution of σ and $\dot{\sigma}$: (a) in case of Disturbance 1; (b) in case of Disturbance 2.

is designed

$$\dot{W}_{\rm ad}(t) = \begin{cases} \gamma_1 |\xi_1(t)| \, \mathrm{sgn}(\xi_1(t)) \, \mathrm{sgn}(\hat{\xi}_2(t)) & \text{if } W_{\rm ad}(t) \geq 0 \\ -\gamma_1 |\xi_1(t)| \, \mathrm{sgn}(\xi_1(t)) \, \mathrm{sgn}(\hat{\xi}_2(t)) & \text{otherwise} \end{cases} \tag{18}$$

where $\hat{\xi}_2$ is determined through (14)-(15), γ_1 is a positive constant arbitrarily set, and $W_{\rm ad}(t_0) = W_{\rm ad_0}$.

Remark 3: In analogy with Remark 1, also in this case the promptness of the adaptation mechanism (18) can be increased adding a term depending on $|\hat{\xi}_2|$, i.e.,

$$\dot{W}_{\rm ad}(t) = \begin{cases} (\gamma_1|\xi_1(t)| + \gamma_2|\hat{\xi}_2(t)|)\,\mathrm{sgn}(\xi_1(t))\,\mathrm{sgn}(\hat{\xi}_2(t)) & \text{if } W_{\rm ad}(t) \geq 0 \\ -(\gamma_1|\xi_1(t)| + \gamma_2|\hat{\xi}_2(t)|)\,\mathrm{sgn}(\xi_1(t))\,\mathrm{sgn}(\hat{\xi}_2(t)) & \text{otherwise} \end{cases} \tag{19}$$

where γ_2 is a positive constant arbitrarily set.

Example

The performance of Strategy 2 can be illustrated making reference again to the academic example (16). Specifically, Figure 7 shows the time evolution of the adaptive gain $W_{\rm ad}$, Figure 8 illustrates the discontinuous control $w(t)$ and the continuous input $u(t)$, while Figure 9 reports time evolution of the sliding variable σ and its first time derivative $\dot{\sigma}$, for both the disturbance instances.

4.3 *Strategy 3*

As shown in (Bartolini et al., 1998a), the estimate of the equivalent control associated with the second order sliding mode control law can be used to compensate the uncertain terms. In fact, only an approximate cancellation of the uncertainties can be performed, which however allows for a reduction of the control effort. In the following, the previous consideration is used to design alternative strategies oriented to improve the performance of Strategies 1 and 2.

Let the discontinuous control input be expressed as

$$w(t) = \gamma_3 w_{\rm ad}(t) + \gamma_4 w_{\rm av}(t) \tag{20}$$

where γ_3, γ_4 are positive definite functions, $w_{\rm ad}$ is chosen as in Strategy 1, that is as indicated in (12) or (13), and $w_{\rm av}$ is the average control obtained at the output of a first order filter having the discontinuous signal $w_{\rm ad}$ as input, i.e.,

$$\tau_1 \dot{w}_{\rm av}(t) + w_{\rm av}(t) = w_{\rm ad} \tag{21}$$

τ_1 being a suitably chosen time constant. Note that, according to the theory introduced in (Utkin, 1992), and the definition of "equivalent control" for systems controlled via SOSM control strategies given in (Bartolini et al., 1998b), $w_{\rm av}$ tends to asymptotically coincide with the equivalent control when a second order sliding mode is established. In this strategy, γ_3 and γ_4 are selected through a weight tuning mechanism analogous to that in (Bartolini et al., 1998a), i.e.,

$$\gamma_3(t) = \begin{cases} 1 & \text{if } |z(t)| \geq 1 \\ |z(t)| & \text{if } \gamma_{3_{\rm min}} < |z(t)| < 1 \\ \gamma_{3_{\rm min}} & \text{if } |z(t)| \leq \gamma_{3_{\rm min}} \end{cases} \tag{22}$$

$$\gamma_4 = 1 - \gamma_3 \tag{23}$$

where z is the output of a first order filter designed as

$$\tau_2 \dot{z}(t) + z(t) = \gamma_3(t)[w(t) - w_{\text{av}}(t)] \tag{24}$$

with τ_2 being a suitably chosen time constant. Note that, the value $\gamma_3 = 1$ corresponds to the case in which only the adaptive discontinuous control law of Strategy 1 is applied. Further, note that $\gamma_{3_{\min}}$ is set on the basis of the various error sources in filtering which can be a priori evaluated. In practice, Strategy 3 tends to coincide with Strategy 1 when the controlled system is far from being in sliding mode. On the other hand, when the sliding mode is almost reached or even enforced, the major component of the control law (20) is the estimate of the equivalent control. The suitable blend between the adaptive SOSM control law of Strategy 1 and its filtered version according to (21) is realized by the peculiar switching logic in (22)-(23).

Example

Consider again the academic example in (16) and apply Strategy 3 with $\gamma_{3_{\min}} = 0.05$, $\tau_1 = 0.5$, $\tau_2 = 10$, and the same parameters used for Strategy 1. Figure 10 reports the time evolution of the adaptive gain W_{ad} for both Disturbance 1 and Disturbance 2, when Strategy 3 is applied. Figure 11 illustrates the discontinuous control $w(t)$ and the continuous input $u(t)$, respectively. Finally, Figure 12 reports the time evolution of the sliding variable σ and its first time derivative $\dot{\sigma}$, for both the disturbances.

4.4 *Strategy 4*

A further adaptive SOSM control strategy can be attained by composing Strategy 2 with the mechanism to estimate the equivalent control described in Strategy 3. Let the discontinuous control input be expressed as in (20), where w_{ad} is chosen as in Strategy 2, i.e., as given by (18) or (19), and w_{av} is the average control obtained as in (21). Moreover, also in this case, γ_3 and γ_4 are selected as in (22)-(24).

Example

Consider again the academic example in (16), and apply Strategy 4. Also in this case $\gamma_{3_{\min}} = 0.05$, $\tau_1 = 0.5$, $\tau_2 = 10$, and the values of the other parameters are those used for Strategy 2. Figure 13 reports the time evolution of the adaptation gain W_{ad} for both the disturbance instances, while Figure 14 illustrates the discontinuous control $w(t)$ and the corresponding continuous input $u(t)$, respectively. Figure 15, finally, reports the time evolution of the sliding variable σ and its first time derivative $\dot{\sigma}$, in both the considered scenarios.

5. Stability Analysis

In this section, the ASSOSM control strategies previously introduced are theoretically analyzed. Explicit theorems are provided for Strategies 1 and 3. Moreover, comments on the stability features of Strategy 2 and 4 are also reported. Note that the proposed adaptive control laws are valid for systems of type (6) with g having known sign. In the considered microgrid case study, $g = 1/L_t$ (see (7)), i.e., it is positive even if L_t is not perfectly known. So, even if hereafter g is assumed to be positive, all the following considerations also hold, with minor changes, for negative g.

Let $\{F_i\}$, $\{G_{1_i}\}$ and $\{G_{2_i}\}$, $i \in \mathbb{N}$ denote the sequences of relative unknown extremal values of

function f and g, such that

$$|F_i| \leq F, \quad G_{1_i} \geq G_1, \quad G_{2_i} \leq G_2 \tag{25}$$

with F being the unknown upper bound of function f, G_1 and G_2 being the unknown lower bound and upper bound of function g, respectively. Let t_{d_i} be the time instants when

$$W_{\text{ad}} > \max\left(\frac{|F_i|}{G_{1_i}}; \frac{4|F_i|}{3G_{1_i} - G_{2_i}}\right), \quad i \in \mathbb{N} \tag{26}$$

and t_d be the time instant when (26) holds, with $|F_i| = F$, $G_{1_i} = G_1$ and $G_{2_i} = G_2$. Moreover, let t_{r_δ} be the time instant when the sliding variable reaches a δ-vicinity of the origin of the auxiliary state-space, and t_r be the time instant when the sliding manifold is finally reached, i.e., $\sigma(t) = 0$, $\dot{\sigma}(t) = 0$, $\forall\, t \geq t_r$.

With reference to the ASSOSM control strategies proposed in the previous section, the following results can be proved.

Theorem 1: *Given the auxiliary system* (6)-(8)*, applying Strategy 1 with the control law* (9)*, the Peak Detection Algorithm and the adaptive mechanism in* (12)*, then, in a finite time $t_{r_\delta} \geq t_d$, the auxiliary system state variables ξ_1 and ξ_2 are ultimately bounded in a δ-vicinity of the origin of the auxiliary system state-space.*

Proof. Two different cases can occur.
Case 1 ($|F_i| = F$, $G_{1_i} = G_1$ and $G_{2_i} = G_2$, for some $i \in \mathbb{N}$): In this case, one can distinguish between two subcases:
Subcase 1.1: $W_{\text{ad}}(t_0) = W_{\text{ad}_0}$ is such that

$$W_{\text{ad}_0} > \max\left(\frac{F}{G_1}; \frac{4F}{3G_1 - G_2}\right) \tag{27}$$

which implies that $t_d = t_0$. Then, since the standard convergence condition for the SSOSM algorithm (Bartolini et al., 1998c) is satisfied, the control law (9) enforces the generation of a sequence of states with coordinates featuring the contraction property expressed by

$$|\xi_{1\max_{i+1}}| < |\xi_{1\max_i}| \tag{28}$$

where $\xi_{1\max_i}$ is the i-th extremal value of variable ξ_1. Considering the Peak Detection Algorithm, and assuming a finite time to evaluate $\xi_1(t)$ and the change of sign of $\Delta(t)$ in (10), in the worst case, the extremal value $\xi_{1\max_i}$ is detected with a delay of $\delta/2$ with respect to the actual time instant $t_{\max_i}$, when $\xi_{1\max_i}$ actually occurs. Consider for the sake of simplicity the case in which the estimate $\hat{\xi}_{1\max_i} > 0$ (the opposite case is specular), and assume to apply (9) with the amplitude $W_{\text{ad}}(t_d) = W_{\text{ad}_0}$ to the auxiliary system (6). In analogy with (Bartolini, Ferrara, and Usai, 1997), one has that

$$\hat{\xi}_{1\max_i} = \xi_{1\max_i} - \left(W_{\text{ad}_0} - \frac{F}{G_1}\right)\frac{\delta^2}{8} \tag{29}$$

Deriving (29), one obtains

$$\hat{\xi}_2 = \xi_2 - \left(W_{\text{ad}_0} - \frac{F}{G_1}\right)\frac{\delta}{4} \tag{30}$$

This means that the actual evolutions of ξ_1 and ξ_2 differ of $\mathcal{O}(\delta^2)$ and $\mathcal{O}(\delta)$, respectively, with respect

to the ideal evolutions. This implies that in a finite time $t_{r_\delta} \geq t_d$ the distance of the sliding variable and its first time derivative from the origin of the auxiliary state-space is of $\mathcal{O}(\delta)$.

Subcase 1.2: $W_{\mathrm{ad}}(t_0) = W_{\mathrm{ad}_0}$ does not satisfy (27). Then, the adaptive mechanism (12) makes the adaptive gain $W_{\mathrm{ad}}(t)$ grow, while the sliding variable increases. This process lasts until time instant $t_{d_i} = t_d$, when the adaptive gain is such that (27) holds. At this point, Subcase 1.1 occurs.

Case 2 ($F_i < F$, $G_{1_i} > G_1$ and $G_{2_i} < G_2$ $i \in \mathbb{N}$): Also in this case two subcases can be distinguished.

Subcase 2.1: $W_{\mathrm{ad}}(t_0) = W_{\mathrm{ad}_0}$ is such that (26) holds. In this subcase, until $|f(\cdot)| \leq |F_i|$ and $G_{1_i} \leq g(\cdot) \leq G_{2_i}$, the control amplitude is sufficient to dominate the uncertain terms, so that a contraction, analogous to that described in (28) for Subcase 1.1, occurs. When $|f(\cdot)| > |F_i|$ and/or $g(\cdot) < G_{1_i}$ or $g(\cdot) > G_{2_i}$, the auxiliary variable $\xi_1(t)$ tends to increase. If $|\xi_1(t)| > |\Xi_{1_{\max}}(t)|$, $\Xi_{1_{\max}}(t)$ as in (11), the adaptive mechanism (12) makes the adaptive gain $W_{\mathrm{ad}}(t)$ grow until the time instant $t_{d_{i+1}}$ when

$$W_{\mathrm{ad}} > \max\left(\frac{|F_{i+1}|}{G_{1_{i+1}}}; \frac{4|F_{i+1}|}{3G_{1_{i+1}} - G_{2_{i+1}}}\right), \quad i \in \mathbb{N} \tag{31}$$

So, a contraction as in (28) occurs again. This mechanism iterates until $F_j = F$, $G_{1_j} = G_1$ and $G_{2_j} = G_2$, $j > i+1$, when Subcase 1.1 occurs.

Subcase 2.2: $W_{\mathrm{ad}}(t_0) = W_{\mathrm{ad}_0}$ does not satisfy (26). Then, $\xi_1(t)$ tends to increase until the time instant t_{d_i} when the adaptive gain W_{ad} is such that (26) holds. At this point, Subcase 2.1 occurs. □

Theorem 2: *Given the auxiliary system* (6)-(8)*, applying Strategy 1 with the control law* (9)*, the adaptive mechanism in* (13)*, and the Levant's Differentiator* (14)-(15)*, assume that* $t_0 \geq t_{Ld}$*,* t_{Ld} *being the finite time necessary for the differentiator convergence, then, in a finite time* $t_r \geq t_d \geq t_0$*, the auxiliary system state variables* ξ_1 *and* ξ_2 *are steered to the origin of the auxiliary system state-space, i.e., a second order sliding mode is enforced.*

Proof. In analogy with Theorem 1, two different cases can occur.

Case 1 ($|F_i| = F$, $G_{1_i} = G_1$ and $G_{2_i} = G_2$, for some $i \in \mathbb{N}$): In this case, one can distinguish between two subcases:

Subcase 1.1: $W_{\mathrm{ad}}(t_0) = W_{\mathrm{ad}_0}$ is such that (27) holds, which implies that $t_d = t_0$. Then, since the standard convergence condition for the SSOSM algorithm (Bartolini et al., 1998c) is satisfied, the control law (9) enforces the generation of a sequence of states with coordinates featuring the contraction property expressed by (28). Since the peak detection device in Figure 2 and the Levant's differentiator (14)-(15) are used, and, by assumption, $t_0 \geq t_{Ld}$, the value of ξ_2 is perfectly known so that the maximum value $\xi_{1_{\max_i}}$ is detected in principle with ideal accuracy. This implies that the auxiliary system state variables reach in a finite time the origin of the auxiliary state-space, and a second order sliding mode is enforced.

Subcase 1.2: $W_{\mathrm{ad}}(t_0) = W_{\mathrm{ad}_0}$ does not satisfy (27). Then, the adaptive mechanism (13) makes the adaptive gain $W_{\mathrm{ad}}(t)$ grow, while the sliding variable increases. This process lasts until time instant $t_{d_i} = t_d$, when the adaptive gain is such that (27) holds. At this point, Subcase 1.1 occurs.

Case 2 ($F_i < F$, $G_{1_i} > G_1$ and $G_{2_i} < G_2$ $i \in \mathbb{N}$): Also in this case two subcases can be distinguished.

Subcase 2.1: $W_{\mathrm{ad}}(t_0) = W_{\mathrm{ad}_0}$ is such that (26) holds. In this subcase, until $|f(\cdot)| \leq |F_i|$ and $G_{1_i} \leq g(\cdot) \leq G_{2_i}$, the control amplitude is sufficient to dominate the uncertain terms, so that a contraction, analogous to that described in (28) for Subcase 1.1, occurs. When $|f(\cdot)| > |F_i|$ and/or $g(\cdot) < G_{1_i}$ or $g(\cdot) > G_{2_i}$, the auxiliary variable $\xi_1(t)$ tends to increase. If $|\xi_1(t)| > |\Xi_{1_{\max}}(t)|$, $\Xi_{1_{\max}}(t)$ as in (11), the adaptive mechanism (13) makes the adaptive gain $W_{\mathrm{ad}}(t)$ grow until the time instant $t_{d_{i+1}}$ when (31) holds. So, a contraction as in (28) occurs again. This mechanism iterates until $F_j = F$, $G_{1_j} = G_1$ and $G_{2_j} = G_2$, $j > i+1$, when Subcase 1.1 occurs.

Subcase 2.2: $W_{\mathrm{ad}}(t_0) = W_{\mathrm{ad}_0}$ does not satisfy (26). Then, $\xi_1(t)$ tends to increase until the time instant t_{d_i} when the adaptive gain W_{ad} is such that (26) holds. At this point, Subcase 2.1 occurs. □

Remark 4: Note that, also in case of Strategy 2, Theorem 1 and Theorem 2 hold. The proofs are analogous to the previous ones, with the difference in the mechanism to tune the amplitude W_{ad}.

Now, by virtue of Theorem 1 and Theorem 2 also the following result can be proved.

Theorem 3: *Given the auxiliary system* (6)-(7)*, applying Strategy 3 with the control law* (20)-(24) *and* (9)*, the Peak Detection Algorithm and the adaptive mechanism* (12)*, then, in a finite time* $t_{r_\delta} \geq t_d$*, the auxiliary system state variables* ξ_1 *and* ξ_2 *are ultimately bounded in a* δ*-vicinity of the origin of the auxiliary system state-space.*

Proof. The proof is analogous to that of Theorem 1, observing that the saturation level $\gamma_3 = \gamma_{3_{\min}}$ in the weight tuning mechanism (22)-(23) corresponds to the fact that the discontinuous control (9) is never switched off, so that it again guarantees, in a finite time $t_{r_\delta} \geq t_d$, the reaching of a δ-vicinity of the sliding manifold. □

Theorem 4: *Given the auxiliary system* (6)-(8)*, applying Strategy 3 with the control law* (20)-(24) *and* (9)*, the adaptive mechanism in* (13)*, and the Levant's differentiator* (14)-(15)*, assume that* $t_0 \geq t_{Ld}$*,* t_{Ld} *being the finite time necessary for the differentiator convergence, then, in a finite time* $t_r \geq t_d \geq t_0$*, the auxiliary system state variables* ξ_1 *and* ξ_2 *are steered to the origin of the auxiliary system state-space, i.e., a second order sliding mode is enforced.*

Proof. The proof is analogous to that of Theorem 2, observing that the saturation level $\gamma_3 = \gamma_{3_{\min}}$ in the weight tuning mechanism (22)-(23) corresponds to the fact that the discontinuous control (9) is never switched off, so that it guarantees that, in a finite time $t_r \geq t_d$ ($t_d \geq t_0 \geq t_{Ld}$), the reaching of the sliding manifold is attained. This is true even if the predominant control component, to reduce the control amplitude in steady-state, is the average control obtained at the output of the first order filter (21). □

Remark 5: Theorems 3 and 4 are valid also for Strategy 4 which differs only for the adaptive mechanism to tune W_{ad}.

As a final comment, note that all the proposed ASSOSM control strategies, independently of the adaptive law adopted, solve Problem 1 when the Levant's differentiator is used, while they solve Problem 2 when they are implemented via the Peak Detection Algorithm.

6. Selection of the ASSOSM Control Strategies to Apply to the Microgrid Case Study

In order to better evaluate the performance of the four strategies and select those to apply to the microgrid case study, we have considered two indices: i) the RMS value of the sliding variable, σ_{RMS}; ii) the control effort, E_c. They are defined as follows

$$\sigma_{RMS} = \sqrt{\frac{\sum_{i=1}^{n_s} \sigma_i^2}{n_s}}, \quad E_c = \sqrt{\frac{\sum_{i=1}^{n_s} u_i^2}{n_s}} \tag{32}$$

where n_s is the number of integration steps during simulations, and σ_i and u_i are the sliding variable and the control variable at the i-th integration step, respectively.

Table 1 reports the performance indices obtained for the four strategies with the two disturbances, when both the transient phases and the steady-state evolution are taken into account. Table 2 reports the performance indices in the case in which only the steady-state is considered. Note that, since the bounds on the uncertain terms are assumed to be unknown, the control gain in all the considered strategies is adaptively tuned whenever a new disturbance, greater in magnitude than previous ones,

Table 1. Performance indices to evaluate the four strategies with Disturbances 1 and 2. Evaluation done also considering transient phases.

Strategy/Index	σ_{RMS}		E_c	
Disturbance	1	2	1	2
1	5.1936	6.7733	12.7915	20.6718
2	6.9745	12.0762	13.6804	45.4156
3	5.1937	6.5806	18.1438	24.1180
4	21.7294	22.3844	101.2887	100.8426

Table 2. Performance indices to evaluate the four strategies with Disturbances 1 and 2. Evaluation done only in steady-state.

Strategy/Index	σ_{RMS}		E_c	
Disturbance	1	2	1	2
1	1.0385×10^{-5}	1.5098×10^{-5}	0.3011	0.3226
2	2.3072×10^{-6}	1.9269×10^{-6}	0.2499	0.2908
3	1.2471×10^{-6}	7.1426×10^{-7}	0.2979	0.3162
4	1.8650×10^{-6}	7.7260×10^{-7}	0.3161	0.3162

affects the system. The sliding variable leaves the sliding manifold, that is a new transient period is observed. The duration of the transient also depends on the choice of the parameters of the adaptive control law. From the comparison, it appears that Strategies 1 and 3 result better than Strategies 2 and 4, both in terms of RMS value of the sliding variable (70% improvement of Strategy 3 with respect to Strategy 4), and of control effort (76% improvement of Strategy 3 with respect to Strategy 4) when also the transient phases are considered (see Table 1). If one considers only the steady-state (see Table 2), while the control energy results in being similar for all the strategies, the RMS value of the sliding variable is better in case of Strategy 3 (8% improvement with respect to Strategy 4). Strategies 2 and 4 give rise to frequent changes of sign of the derivative of the adaptive gain which could introduce harmonics distortions in current and voltage profiles, possibly making the load supply impracticable and violating the IEEE recommendation for power systems (IEEE, 2009). Thus, having in mind the application to the microgrids, where the transient phases can be frequent (especially in case of load variations, exogenous disturbances, and disconnection/reconnection to the main grid), and steady-state tracking accuracy is required, Strategy 1 and 3 appear to be the most adequate. Note that Strategy 2 and Strategy 4 do not appear suitable for the considered microgrid (this could be also due to the difficulties to determine the ideal parameters tuning). Anyway, they could be of interest for other applications even of electrical type.

7. Application of the Selected ASSOSM Control Strategies to the Microgrid Case Study

In this section, Strategy 1 and Strategy 3 are verified in simulation by applying them to the model of a DGu. Moreover, in order to show the advantages of the proposed methods, a conventional PI control has been also applied and tuned relying on the standard Ziegler-Nichols method (Ziegler and Nichols, 1942), to obtain a satisfactory behaviour of the controlled system such that the control effort is almost equal to the smallest one between Strategy 1 and Strategy 3. The nominal values of the electrical parameters of the DGu considered in the tests (see Figure 1) are reported in Table 3, while the parameters of the proposed control strategies are indicated in Table 4, in which it is assumed that $t_0 = 0\,\mathrm{s}$, and $W_{\mathrm{ad},d}(0)$, $W_{\mathrm{ad},q}(0)$ are chosen relying on an estimate of the upper bounds of (7)-(8), in order to dominate the uncertain terms. In simulation the electrical parameters have been set to values which differ from the nominal values of an additive 10%. From $t = 0.05\,\mathrm{s}$ to $t = 0.1\,\mathrm{s}$ a matched disturbance u_{VSC_q} with trapezoidal shape and maximum value equal to $3 \times 10^3\,\mathrm{V}$

Table 3. Electrical parameters of the DGu.

Quantity	Value	Description
V_{DC}	1000 V	DC voltage source
f_c	10 kHz	PWM carrier frequency
R_t	40 mΩ	VSC filter resistance
L_t	10 mH	VSC filter inductance
R	4.33 Ω	Load resistance
L	100 mH	Load inductance
C	1 pF	Load capacity
R_s	0.1 Ω	Grid resistance
f_0	60 Hz	Nominal grid frequency
$V_{n_{RMS}}$	120 V	Nominal grid phase-voltage
$I_{td,ref}$	60 A	d-component of current ref.
$I_{tq,ref}$	0 A	q-component of current ref.

Table 4. Parameters

Parameter	Value
$W_{\mathrm{ad},d}(0) = W_{\mathrm{ad},q}(0)$	4.5×10^7
$\gamma_{1,d} = \gamma_{2,d}$	5.0×10^7
$\gamma_{1,q} = \gamma_{2,q}$	5.0×10^5
$\tau_{1_d} = \tau_{1_q}$	0.5×10^3
$\tau_{2_d} = \tau_{2_q}$	10×10^3
$\gamma_{3_{\min},d} = \gamma_{3_{\min},q}$	$1/35$
$K_{P_d} = K_{P_q}$	30
$K_{I_d} = K_{I_q}$	2×10^3

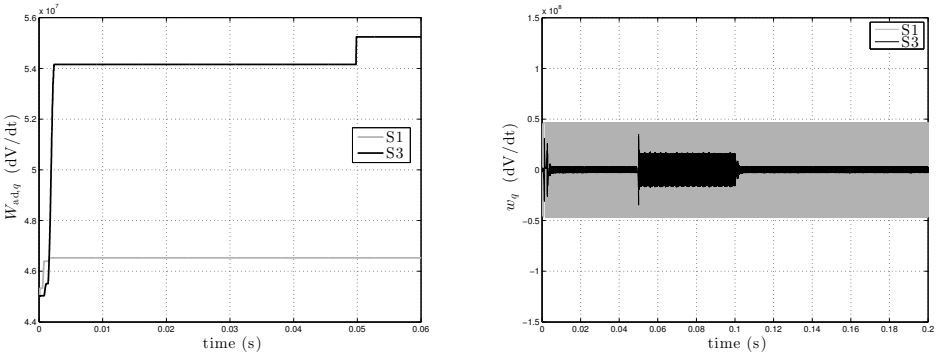

(a) (b)

Figure 16. Comparison between Strategies 1 and 3: (a) adaptive gain $W_{\mathrm{ad},q}$; (b) discontinuous control w_q.

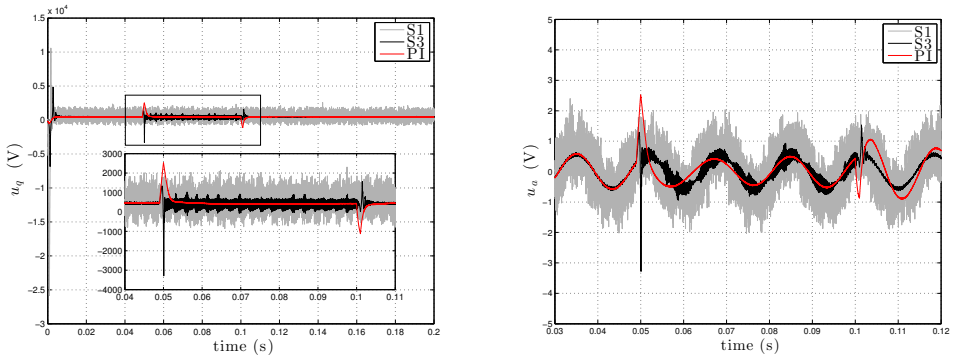

(a) (b)

Figure 17. Comparison between Strategies 1 and 3: (a) continuous input u_q; (b) modulating voltage signal u_a of phase a.

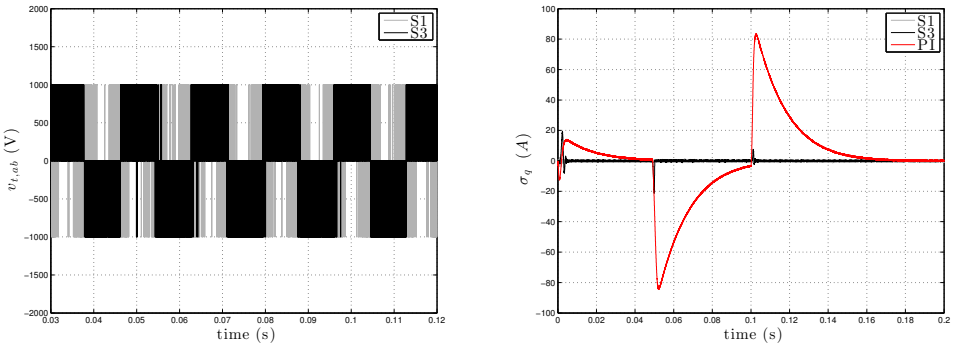

Figure 18. Comparison between Strategies 1 and 3 and PI control: (a) phase-to-phase VSC output voltage $v_{t,ab}$; (b) error signals σ_q.

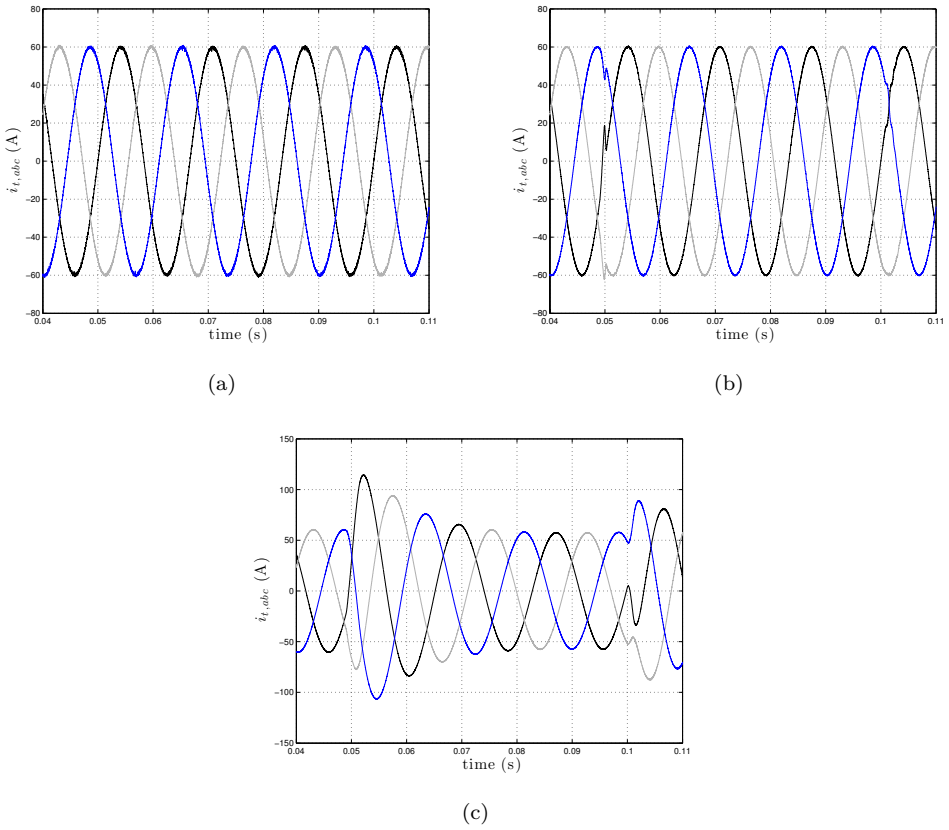

Figure 19. Instantaneous three-phase current delivered by the DGu in presence of a matched disturbance: (a) Strategy 1; (b) Strategy 3; (c) PI control.

acts on the same channel of the input u_q. The trapezoidal shape is justified by the assumption on the Lipschitz continuity of the disturbance signals. The discretization interval is $T_s = 1 \times 10^{-6}$ s and the simulation time is $T_f = 0.2$ s.

Figure 16 shows, both for Strategy 1 (S1) and Strategy 3 (S3), the time evolution of the adaptive gain $W_{\mathrm{ad},q}$, and the discontinuous control variable w_q. Note that, since the gain W_{ad} cannot decrease according to Strategy 1 and Strategy 3, the decreasing of the gain is due to the adaptation law (20). Figure 17 reports the continuous input u_q, and the modulating signal u_a of the phase a to

Table 5. Performance indices to evaluate Strategy 1 and Strategy 3. Evaluation done also considering transient phases.

Strategy/Index	$\sigma_{RMS,q}$	$E_{c,q}$	THD
1	0.3680	1385.5	0.0104
3	1.5408	528.92	0.0224
PI	26.46	489.81	0.1831

Table 6. Performance indices to evaluate Strategy 1 and Strategy 3. Evaluation done only in steady-state.

Strategy/Index	$\sigma_{RMS,q}$	$E_{c,q}$	THD
1	0.3116	737.40	0.0087
3	0.2161	446.21	0.0047
PI	1.28	460.30	0.0129

apply the PWM technique, while Figure 18 shows the phase-to-phase VSC output voltage $v_{t,ab}$ and the sliding variable σ_q, i.e., the error of I_{tq} with respect to the corresponding reference $I_{tq,ref}$. Note that, when Strategy 3 is implemented, then the typical PWM waveform of the phase-to-phase VSC output voltage (see Figure 18 (a)) is obtained with a smaller number of switchings, which implies lower IGBTs energy losses. In Figure 19 the instantaneous three-phase currents delivered by the DGu, by applying Strategy 1, Strategy 3 and PI control, respectively, are compared.

In order to quantitatively compare the selected strategies when they are applied to the microgrid case study, the performance indices in (32) are used. They are reported, together with the Total Harmonics Distortion (THD) index (Mohan et al., 2003), in Table 5 including in the evaluation also the transients phases and, in Table 6 considering for the evaluation only the steady-state. Considering also the transient phase, Strategy 1 results better than Strategy 3 and PI in terms of RMS value of the sliding variable (76% and 98.61% improvement), and THD (54% and 94% improvement). In terms of control energy, PI control is more performant (65% and 7% improvement). If one considers only the steady-state, Strategy 3 results in being the most effective in terms of RMS value of the sliding variable (31% and 83% improvement), while the PI in terms of control energy (38% and 3% improvement). Strategy 3 is the better also in terms of THD (46% and 64% improvement). On the whole, both Strategies 1 and 3 are effective and satisfactory, but the one which appears most performing in all the situations is Strategy 3.

8. Conclusions

In this paper, adaptive second order sliding mode control strategies based on the Suboptimal algorithm have been presented for a class of uncertain systems with unknown uncertainty bound. Four strategies have been designed and analyzed. They adjust the amplitude of the control law in order to dominate the uncertain terms and enforce the attainment of a second order sliding mode, or the convergence of the auxiliary system state variables to a vicinity of the origin in a finite time. The first two strategies are purely adaptive versions of the basic Suboptimal algorithm, while the other two, in order to reduce the control amplitude, exploit a well-balanced blend between two control components: one mainly working during the reaching phase, the other being the predominant one in a vicinity of the sliding manifold. In the paper, the proposed adaptive second order sliding mode control strategies have been compared taking into account the tracking accuracy and the control effort. Two strategies have been selected as the most appropriate to be applied to the microgrid case study. The performance of the selected adaptive control laws have been satisfactorily assessed in simulation by considering a DGu model in realistic scenarios, characterized by disturbances and

parameters variations.

References

M. Babazadeh and H. Karimi. Robust decentralized control for islanded operation of a microgrid. In *Proc. IEEE Power and Energy Society General Meeting*, pages 1–8, Jul. 2011a.

M. Babazadeh and H. Karimi. μ-synthesis control for an islanded microgrid with structured uncertainties. In *Proc. 37th IEEE Conf. Ind. Electron. Society*, pages 3064–3069, Nov. 2011b.

G. Bartolini, A. Ferrara, and E. Usai. Output tracking control of uncertain nonlinear second-order systems. *Automatica*, 33(12):2203 – 2212, Dec. 1997.

G. Bartolini, A. Ferrara, A. Pisano, and E. Usai. Adaptive reduction of the control effort in chattering-free sliding-mode control of uncertain nonlinear systems. *Int. J. Applied Mathematics and Computer Science*, 8:51–57, Jan. 1998a.

G. Bartolini, A. Ferrara, and E. Usai. On boundary layer dimension reduction in sliding mode control of siso uncertain nonlinear systems. In *Proc. IEEE Int. Conf. Control Applications*, volume 1, pages 242 –247 vol.1, Trieste, Italy, Sep. 1998b. .

G. Bartolini, A. Ferrara, and E. Usai. Chattering avoidance by second-order sliding mode control. *IEEE Trans. Automat. Control*, 43(2):241–246, Feb. 1998c.

G. Bartolini, A. Ferrara, E. Usai, and V.I. Utkin. On multi-input chattering-free second-order sliding mode control. *IEEE Trans. Automat. Control*, 45(9):1711–1717, Sep. 2000.

I. Boiko, L. Fridman, A. Pisano, and E. Usai. Analysis of chattering in systems with second-order sliding modes. *IEEE Trans. Automat. Control*, 52(11):2085–2102, Nov. 2007.

M. Cucuzzella, G. P. Incremona, and A. Ferrara. Master-slave second order sliding mode control for microgrids. In *Proc. IEEE American Control Conf.*, Chicago, IL, USA, Jul. 2015a.

M. Cucuzzella, G. P. Incremona, and A. Ferrara. Third order voltage control of microgrids. In *Proc. IEEE European Control Conf.*, Linz, Austria, Jul. 2015b.

M. Cucuzzella, G. P. Incremona, and A. Ferrara. Design of robust higher order sliding mode control for microgrids. *IEEE J. Emerg. Sel. Topics Circuits Syst.*, 5(3):393–401, Sep. 2015c.

K. De Brabandere, B. Bolsens, J.. Van den Keybus, A. Woyte, J. Driesen, and R. Belmans. A voltage and frequency droop control method for parallel inverters. *IEEE Trans. Power Electron.*, 22(4):1107–1115, Jul. 2007.

F. Dinuzzo and A. Ferrara. Higher order sliding mode controllers with optimal reaching. *IEEE Trans. Automat. Control*, 54(9):2126 –2136, Sep. 2009.

C. Edwards and S. K. Spurgeon. *Sliding Mode Control: Theory and Applications*. Taylor and Francis, London, UK, 1998.

A. Ferrara and G. P. Incremona. Design of an integral suboptimal second-order sliding mode controller for the robust motion control of robot manipulators. *IEEE Trans. Control Syst. Technol.*, PP(99):1, May 2015.

L. Fridman. The problem of chattering: an averaging approach. In K.D. Young and Ü. Özgüner, editors, *Variable structure systems, sliding mode and nonlinear control*, volume 247 of *Lecture Notes in Control and Information Sciences*, pages 363–386. Springer London, 1999.

L. Fridman. Singularly perturbed analysis of chattering in relay control systems. *IEEE Trans. Automat. Control*, 47(12):2079–2084, Dec. 2002.

M. Hamzeh, H. Karimi, and H. Mokhtari. A new control strategy for a multi-bus mv microgrid under unbalanced conditions. *IEEE Trans. Power Syst.*, 27(4):2225–2232, Nov. 2012.

M. Hamzeh, A. Ghazanfari, H. Mokhtari, and H. Karimi. Integrating hybrid power source into an islanded mv microgrid using chb multilevel inverter under unbalanced and nonlinear load conditions. *IEEE Trans. Energy Convers.*, 28(3):643–651, Sep. 2013.

J. Han, S.K. Solanki, and J. Solanki. Coordinated predictive control of a wind/battery microgrid system. *IEEE J. Sel. Topics Power Electron.*, 1(4):296–305, Dec. 2013.

IEEE. Recommended practice for monitoring electric power quality. *IEEE Std 1159-2009 (Revision of IEEE Std 1159-1995)*, pages c1–81, Jun. 2009.

A. Isidori. *Nonlinear Control Systems*. Springer Verlag, New York, 1995.

H. Karimi, H. Nikkhajoei, and R. Iravani. Control of an electronically-coupled distributed resource unit subsequent to an islanding event. *IEEE Trans. Power Del.*, 23(1):493–501, Jan. 2008.

R.H. Lasseter. Microgrids. In *Proc. IEEE Power Engineering Society Winter Meeting*, volume 1, pages 305–308, 2002.

R.H. Lasseter and P. Paigi. Microgrid: a conceptual solution. In *Proc. 35th IEEE Power Electron. Specialists Conf.*, volume 6, pages 4285–4290 Vol.6, Jun. 2004.

C-.T. Lee, C-.C. Chu, and P-.T. Cheng. A new droop control method for the autonomous operation of distributed energy resource interface converters. *IEEE Trans. Power Electron.*, 28(4):1980–1993, Apr. 2013.

A. Levant. Robust exact differentiation via sliding mode technique. *Automatica*, 34(3):379–384, Mar. 1998.

A. Levant. Higher-order sliding modes, differentiation and output-feedback control. *Int. J. Control*, 76 (9-10):924–941, Jan. 2003.

N. Mohan, T. M. Undeland, and W. P. Robbins. *Power Electronics: Converters, Applications, and Design*. Power Electronics: Converters, Applications, and Design. John Wiley & Sons, 2003.

A. Ouammi, H. Dagdougui, L. Dessaint, and R. Sacile. Coordinated model predictive-based power flows control in a cooperative network of smart microgrids. *IEEE Trans. Smart Grid*, PP(99):1–1, Sep. 2015.

O. Palizban, K. Kauhaniemi, and J. M. Guerrero. Microgrids in active network management—part i: Hierarchical control, energy storage, virtual power plants, and market participation. *Renewable and Sustainable Energy Reviews*, 36(0):428 – 439, Aug. 2014.

A. Parisio, E. Rikos, and L. Glielmo. A model predictive control approach to microgrid operation optimization. *IEEE Trans. Control Syst. Techn.*, 22(5):1813–1827, Sep. 2014.

R. H. Park. Two-reaction theory of synchronous machines - generalized method of analysis - part i. *Trans. American Instit. Electr. Eng.*, 48(3):716 – 727, Jul. 1929.

A. Pisano, M. Tanelli, and A. Ferrara. Switched/time-based adaptation for second-order sliding mode control. *Automatica*, 64:126–132, Dec. 2015.

E. Planas, A. Gil-de Muro, J. Andreu, I. Kortabarria, and I. M. de Alegría. General aspects, hierarchical controls and droop methods in microgrids: A review. *Renewable and Sustainable Energy Reviews*, 17(0): 147 – 159, Jan. 2013.

Y. Shtessel, C. Edwards, L. Fridman, and A. Levant. Higher-order sliding mode controllers and differentiators. In *Sliding Mode Control and Observation*, pages 213–249. Springer, 2014.

Y. B. Shtessel, L. Fridman, and A. Zinober. Higher order sliding modes. *Int. J. Robust and Nonlin. Control*, 18(4-5):381–384, Mar. 2008.

V. I. Utkin. *Sliding Modes in Optimization and Control Problems*. Springer Verlag, New York, 1992.

J. G. Ziegler and N. B. Nichols. Optimum settings for automatic controllers. *ASME. J. Dyn. Syst.*, 64(759), Nov. 1942.